TITLE

Column tests investigating the liquefaction of partially saturated loose non-plastic soils

AUTHORS

K.A Kwa[1], Y. Hu[1], J. Chen[1], Z. Chen[2] & D.W Airey[1]

[1]School of Civil Engineering, University of Sydney

[2]School of Civil Engineering, Shaoxing University, Shaoxing, Zhejiang 312000, China

ABSTRACT

This study reports data and findings from shake table tests performed on loosely compacted unsaturated well graded materials containing a wide range of particle sizes and significant fines contents of 18 to 28%. The results are useful for understanding the fundamental cyclic liquefaction behaviour of these unsaturated well graded materials when subjected to vertical cyclic loading conditions relevant to repetitive transport loading or during bulk cargo shipping transportation. Liquefaction was observed in all the shake table tests performed on the well-graded materials, which were prepared at relative densities of 50 to 60% and degrees of saturation ranging from 50% to 70%. Large settlements were also observed in the columns of the well-graded materials, which resulted in significant increases in the degree of saturation towards fully saturated states. Migration of fines throughout the well-graded materials was also observed, which also contributed to settlement and resulted in different local densities and fines contents throughout the column. The resulting build-up in pore pressures, settlements and accompanying increases in degree of saturation and movement of moisture throughout are presented and compared with shake table tests performed on columns of partially saturated clean sand for which liquefaction was not observed.

1. INTRODUCTION

There is relatively limited data that describes the cyclic response of partially saturated soils as studies have mainly focused on the cyclic response of either fully dry or fully saturated materials. Traditionally, the worst cyclic soil responses are expected when the soil is either fully dry, and large settlements occur, or the soil is completely saturated, and there is a large build up in pore pressure and decrease in effective stress. The consensus that soils with intermediate degrees of saturation result in less critical behaviour due to the role of matric suctions, has lately been questioned (Ghayoomi and McCartney, 2012). In recent years there has been increasing interest in the seismic response of partially saturated soils as during earthquake events they have been associated with significant compression (Stewart and Whang, 2003, Duku et al, 2008, Ghayoomi et al, 2011) and have been involved in liquefaction failures (Uzuoka et al, 2014; Okamura & Soga, 2006; Unno et al, 2008). Given that partially saturated soils also underlie much of the world's infrastructure, there is an evident need for well documented laboratory and field data to better understand their behaviour and to support rigorous risk assessment. Although there have been many recent studies of the cyclic behaviour of unsaturated soils in simple shear and triaxial tests there are limited data suitable to assess and validate the response of sophisticated numerical models for dynamic unsaturated behaviour. To address this deficiency, shake table tests on columns of partially saturated material have been performed in this study.

Background

It is well known that particle grading has an important influence on the susceptibility to liquefaction and that sands and silty sands are the most prone (Tsuchida, 1970). A large number of element tests, specifically investigating the effect of fines on the saturated cyclic liquefaction response of silty sands have been performed in the triaxial and simple shear apparatuses (Bouckovalas et al., 2003; Dash & Sitharam, 2009; Polito & Martin, 2011; Sadek & Saleh, 2007; Sadrekarimi 2013; Xenaki and Athanasopoulos, 2003; Carrera et al., 2011). There has been much less focus on the cyclic liquefaction behaviour of well-graded materials containing larger gravel sized particles, as these materials do not tend to liquefy as often as sands and silty sands. This is because these materials typically have higher permeabilities and therefore, are able to dissipate pore water pressures more quickly.

Nevertheless, a number of triaxial tests have been performed on saturated and unsaturated well-graded materials (Kimoto et al., 2011; Okamura & Soga, 2006; Unno et al, 2006; 2008, Uzuoka et al, 2014 Wang et al., 2015; Kwa & Airey, 2017; 2019), with a few specifically investigating the effect of fines on the cyclic liquefaction response of unsaturated well-graded materials (Unno et al, 2006; Kwa & Airey, 2017, 2019). If a significant amount of fines is present, the fines have been known to decrease these materials' drainage potential, resulting in cases where materials, containing gravel sized particles, used for reclaimed fill purposes have liquefied during earthquakes (Harder, 1997; Andrus, 1995; Cubrinovski et al, 2003, 2017). The migration of fines from the subgrade into railway ballast and highway pavements due to train and car traffic cyclic loading conditions is also known to reduce the drainage potential of ballast and pavement material, resulting in ballast and pavement degradation and large settlements of the infrastructure above (Alobaidi et al., 1996; Indraratna et al., 2011 Duong et al., 2014; Ebrahimi et al., 2014). Metallic ore bulk cargoes are another material containing a wide range of particle sizes from gravels down to silts and significant fines contents, as high as 28%, that are susceptible to liquefaction during shipping transportation when subjected to rocking motions from sea waves (IMSBC, 2013; Kwa & Airey, 2019). Due to the loading process, these metallic ores are in a relatively loose and in a partially saturated state when placed in the hold of the ship. If they liquefy during transportation, they can cause the ship to progressively tilt, become unstable and then capsize.

The mechanics leading to liquefaction of these unsaturated, well-graded materials, which are widely used as reclaimed fill materials, railway ballast, pavement subbase materials, and are also similar in grading to a number of shipped metallic ores, is not well understood. One of the main challenges is in understanding the settlements, associated increases in the degree of saturation and migration of moisture throughout the partially saturated material when they are subjected to cyclic loads.

Shake table tests are relatively simple model tests that have been widely used to model the 1g saturated behaviour of sands when subjected to seismic loading conditions. In particular, shake tables have been used to investigate the pore pressure responses and 1D settlements in sands (Yanagisawa, 1995; Yegain et al., 2006, 2007; Ueng et al., 2006, 2010, 2017; Pathak et al, 2010, 2013) and to model the displacements and strains of embankments and shallow foundations in sands (Koga et al., 1990; Toyota et al., 2004; Sadrekarimi, 2013). In all of these shake table studies, increases in pore water pressures and significant settlements were measured and reported once liquefaction had occurred. Some studies also measured and observed an upwards flow of water and propagation of pore water pressures throughout column of soil towards the surface once liquefaction had occurred (Ueng et al., 2017; Yang., 2017). Some studies, including those performed by Kokusho (1999), Kokusho et al. (2002) and Ozener et al. (2009), used shake table apparatuses to investigate pore water pressure generation in sand with silts. However, in these studies, shaking was horizontal, and the silt and sand were separated into layers and the effects of interlaying silt within a column of sand were investigated to determine their effect on the upward flow of pore water.

Very few shake table tests have been reported on well-graded materials containing a mixture of particles sizes from gravels down to silts. Shaking has also typically been applied to samples in the horizontal direction, which is less relevant when modelling the cyclic soil response underneath pavements and railway ballast subjected to repetitive vertically acting transport loading conditions, or in metallic ore cargoes during shipping transportation. Some shake table tests and numerical analyses have been performed on unsaturated well-graded samples of iron ore fines (TWG, 2013, Munro & Mohajerani, 2016, Ju et al., 2016) to observe whether the material lost its strength and flowed when subjected to cyclic loads relevant to ship rocking motions, but only limited experimental pore pressure and displacement data have been reported.

More 1g model tests that are better instrumented are required to gain a better understanding of the cyclic liquefaction response of well-graded materials, that contain a wider range of particle sizes than sands and are also prone to liquefaction. This study continues to investigate the cyclic unsaturated liquefaction response of well-graded materials which contain significant fines contents. To gain a more holistic understanding of the build-up in pore pressures, settlements and accompanying increases in the degree of saturation and movement of moisture throughout the material, shake table tests will be performed on columns of loosely compacted, unsaturated well-graded materials containing 18% and 28% fines. This study follows on from other tests which investigated ship cargo liquefaction on well graded materials with a significant fines content, similar in grading and relative densities to iron ore fines (Kwa & Airey, 2019) and the results have been supplemented by tests using a clean sand.

2. METHOD

2.1 Materials

Tests have been performed using Sydney Sand and reconstituted well-graded materials consisting of angular basalt aggregates ranging in particle size from 9.5mm down to 0.015mm mixed with feldspar fines. Grading curves for the sand, feldspar fines and the reconstituted materials are shown in Figure 1. Fines contents of 18% and 28% were used for the reconstituted materials to produce grading curves representative of the lower and upper bound grading curves for iron ore fines (TWG, 2013) and they were also similar in grading to the gravelly fills that were reported to liquefy in Cubrinovski et al. (2003, 2017). The critical state soil parameters and specific gravities for these materials that were obtained in a previous study (Kwa et al., 2019, 2017), are summarised in Table 1.

2.2 Experimental Set up and Sample Preparation

A photograph of the shake table apparatus and Perspex column used to contain the soil are shown in Figure 2. The shake table used in this study is normally used for minimum and maximum density tests according to Australian Standard AS1289.5.5.1 and has a fixed frequency of 50Hz and produces a regular pulsed waveform with peak vertical accelerations of approximately 0.4g, similar to the peak accelerations measured in the cargo of bulk ore carriers. An accelerometer was attached to the base of the shake table. A typical displacement waveform derived from the acceleration data is shown in Figure 3. A 500mm tall by 140mm diameter Perspex column was also fastened onto the shake table and three pressure transducers and three ECHO EC-5 moisture content probes were located at depths of 125mm, 250mm and 375mm from the top of the column. The pressure transducers, moisture content probes and accelerometer were connected to a Vishay System 6000 data acquisition system, capable of measuring up to 4000 readings per second and data were displayed and recorded on a computer.

The pressure transducers were calibrated using a GDS pressure controller. They were cleaned and filled with de-aired water before each test and then were screwed horizontally into the side of the column. Coarse gauze was also placed over the aperture of the transducers to prevent fines from flowing into the transducer. After each test was completed, the transducers were also observed to be filled with clean water, suggesting that they remained saturated throughout the test. Calibration of the moisture content probes was conducted to determine the relation between voltage and moisture content. Tests were performed over the range of expected void ratios and moisture contents for both materials. Figure 4 summarises the calibration curves for the Echo EC-5 moisture content probes in sand and in the well-graded materials tested in this study. The calibration curve for Sydney Sand was consistent with the calibration curves previously obtained in other studies (Campbell, 2001; Tehrani, 2016). However, the calibration curve for the well-graded material was noticeably different, particularly at higher moisture contents. The calibration in the well-graded materials was obtained by using two different methods labelled as wetting and drying in Figure 4. The moisture content within the material was either increased by adding and mixing known amounts of water into the soil (wetting), or they were decreased through allowing the soil to dry out and the mass of water which evaporated out of the soil was measured (drying). The calibration was not sensitive to whether the well-graded materials was subjected to wetting or drying, and the calibration was also not observed to vary significantly with changes in the density of the well-graded materials, as can also be seen in Figure 4.

An unsaturated column of soil was prepared by initially mixing the dry material with water at the required moisture content. Once the moist material was well mixed, it was divided by mass into 10 equal portions. Each portion or layer was subsequently compacted into the column using the same compaction energy per layer to achieve the target relative densities and degrees of saturation for the unsaturated sample. In the columns of pure sand, samples were prepared at void ratios from 0.57 to 0.82 and degrees of saturation ranging from 29% to 68%. In the well-graded materials, the target relative densities and degrees of saturation were relevant to those that have been measured in metallic ore bulk cargoes when loaded into the hold of a ship (TWG, 2013). This corresponded to target void ratios of 0.38 to 0.55 for the well-graded materials containing 18 and 28% fines and degrees of saturation ranging from 50 to 70%. The effects of independently varying the initial dry densities of samples on the unsaturated liquefaction response of these materials were not investigated in this study. Table 2 summarises the individual test conditions, including their global initial and final void ratios, moisture contents and the resulting degrees of saturation and relative densities. In some of the tests, coloured sand was placed between the compacted layers around the container boundary to enable settlement profiles with time to be tracked using photography. Once the column was filled, the shake table was turned on and the soil was subjected to shaking, with drainage only from the upper surface, for 5 to 10 minutes, until the settlement and pore pressures were observed to stabilise.

3. RESULTS & DISCUSSION

3.1 Sand

The settlements measured in the columns of sand during shaking were small and consistent with results from shaking table tests on saturated sand (Ozener et al., 2008). Figure 5 shows the moisture contents measured at the top, middle and bottom of the columns of unsaturated sand during shaking. The initial moisture contents measured at the bottom of the sand column were higher than the moisture contents used during preparation of the sand column and they were also significantly higher than the moisture contents measured at the top of the soil column. This is because water tended to redistribute towards the bottom of the column during preparation as sand is a relatively free draining material. After the water redistributed towards the bottom of the column, the moisture contents remained relatively constant during shaking and liquefaction was not observed despite large numbers of cycles. However, only a limited range of relative densities and initial degree of saturation have been tested and liquefaction may have occurred if the columns of sand with low relative density had been tested at higher degrees of saturation.

3.2 Well graded materials

3.2.1 Settlements

Liquefaction was observed in all the shake table tests performed on the well-graded materials containing 18% and 28% fines. Total settlements of 50mm to 75mm were observed in the columns of the well-graded materials with initial degrees of saturation from 50% to 70%. Additional tests prepared with the same compaction energy at higher initial degrees of saturation, and hence density, resulted in lower settlements (Hu and Chen, 2017). In all tests shaking resulted in decreases in the global void ratios and increases in degree of saturation, towards fully saturated states, with the final water level observed to be at, or above, the surface of the soil. Figure 6 shows settlement profiles during shaking for a test with 28% fines, 28Sr60b. These profiles were obtained by measuring the changes in height of the coloured sand layers as the test progressed. It shows that settlement in the first 30 seconds occurs mostly in the upper 150 mm of the column and as shaking continues the zone where settlement dominates moves downwards. In the first 120 seconds, minimal settlement occurs in the bottom 100 mm, however between 120 and 300 seconds most of the settlement derives from this zone. The coloured layers of sand became difficult to distinguish as the material liquified and after 20 minutes of shaking could not be seen so only the position of the column surface is shown in Figure 6 at the end of the test.

All tests with a given fines content approached similar ultimate states with the final settlement experienced by the soil column dependent on the initial density, a reduction in the initial density resulted in larger settlements.

3.2.2 Pore pressures

Figures 7 and 8 show typical, average pore pressure responses during shaking measured at the top, middle and bottom of the column containing the well-graded materials with 18% and 28% fines. The detailed pore pressure responses could not capture the initial matric suctions and show variable and erratic responses which may have been affected by the cylinder walls and possibly fines slowing down the responses. Nevertheless, these effects do not appear to have influenced the mean pore pressures which rise rapidly once shaking commences. As expected, the highest average pore water pressures were measured at the bottom of the column, followed by the middle and top. Larger oscillations in the pore water pressures were measured in the material containing 18% fines, particularly towards the end of the test, which are believed to be a result of the material being more dilative and having a larger friction angle than the material containing 28% fines (Kwa and Airey, 2017). The average pore pressures during shaking measured at the middle and bottom of the column approached values that were slightly, 0.5 to 3kPa, higher than hydrostatic pressure, taking the water level at the surface of the soil column, implying an upwards flow of water. The pore pressures rose more quickly in samples prepared at higher degrees of saturation and tended closer toward the estimated total stress (calculated assuming material saturated), possibly because there was less air present in the soil.

At all depths the average pore pressures increased and approached the estimated total stresses, which are indicated on the Figures. The rate of pore pressure increase depends on the magnitude of cyclic stresses, increases with the degree of saturation and is limited by drainage. Initially, as a result of the air present in the upper part of the column, the ability of water to flow upward is limited, contributing to the increase of water pressures within the column. As a result, the effective stresses within the soil column tended towards zero and the soil became liquefied. This state of very low effective stress was reached early in the shaking process at the base of the column and migrated upwards as the saturation front rose through the column, which is also evident in the moisture content responses.

3.2.3 Moisture contents

Typical moisture content variations during shaking of the column for material with 28% fines are shown in Figure 9. The initial values indicate moisture redistribution has occurred with moisture contents in the top of the column lower than the as-compacted state. Once shaking commences, there is a small delay before the moisture contents increase at the middle sensor, and after a further delay upper sensor, as the saturation front progressively moves towards the top of the column. This is consistent with the pore pressure increases and accompanying decreases in effective stress which approached zero throughout the whole column once the saturation front reached the surface of the column. Air bubbles in the soil column were also observed to move towards the top of the column during shaking. Spikes in the moisture content readings were caused by small voids forming underneath the moisture content probes which restricted settlements in the surrounding material. This was most noticeable at the top of the column where most of the settlements occurred rapidly at the beginning of the test. However, as the test progressed more constant moisture contents were measured as the saturation degree increased and the material liquefied so that it was able to flow more easily around the probes. The final moisture contents measured at the end of the tests have been summarised in Table 3 and it is evident that the moisture contents measured at the top of the sample were consistently higher than the moisture contents measured at the middle and bottom of the column. This behaviour can be contrasted with the sand tests where moisture content increased with depth following equilibration and then remained essentially unchanged during shaking.

By combining the volume changes for test 28Sr60b and the moisture content responses for test 28Sr62, shown in Figures 6 and 9 respectively, schematic moisture and density paths for the soil at the lower and upper moisture sensor locations can be estimated as shown in Figure 10. The densities associated with e_{max} and e_{min} and the modified Proctor compaction curve, which had a maximum dry density of 2.17t/m^3, are also shown on Figure 10 to aid interpretation. Initially the soil is compacted into the column at a known moisture content (11.5%) to a controlled density with $S_r \approx 61\%$, which is represented by point 1. Moisture redistribution then occurs with water moving to the base of the column with minimal change in volume so that the soil states move to points 2 and 5 for the lower and upper sensor elevations, respectively. There is a smaller decrease in the moisture content measured at the bottom transducer where the moisture content dropped to 9% (point 2) compared to the top transducer, where the moisture content dropped to 3% (point 5).

When shaking commences the moisture content at the bottom transducer location increases rapidly to about 14% in 5 seconds and then remains approximately constant. This peak can be interpreted as the passing of the saturation front. As indicated by the settlement profiles this is not associated with significant volume change and the soil state moves from point 2 to point 3 where it remains for approximately 120 seconds until the saturation front reaches the top of the column. Subsequently water flowed from the base and this was accompanied with a volume strain of 0.125 in the bottom third of the column, resulting in the state moving from point 3 to point 4. The final density is greater than given by e_{min} as a result of an upwards migration of fines associated with the flow of water, discussed further below. At the top transducer location, the column initially experiences unsaturated compression, and within 30 seconds of shaking, the upper one third of the column has an average volume strain of ~0.12, and the soil state moves from point 5 to point 6 without significant change in moisture content. The rising saturation front then causes a gradual rise in moisture content to around 12% at 200 seconds, which is accompanied by a slight loosening in the soil and the soil state moves from point 6 to point 7. As the test progressed, the moisture content gradually continued to rise, and the soil loosened due to the upward flow of water and increasing fines content until the end of the test, at point 8.

Similar trends were observed in the other tests. More rapid rises of the saturation front and increases in the degrees of saturation were observed in tests performed with higher initial degrees of saturation. This can be seen, for example, in comparison of Figure 9a where the initial degree of saturation was 62% and Figure 9b, where initial degree of saturation was 72%.

3.2.4 Migration of fines

The fines in the well-graded materials were observed to migrate towards the surface of the column and a thin layer of fines could be seen lying at the top of the soil column after shaking as shown in Figure 11. A sieve analysis was performed after shaking on four sub-samples that were cut from different parts of the soil column and the resulting grading curves for each sub-sample, labelled as A, B, C and D, are shown in Figure 12. The resulting distributions of fines throughout the column after shaking have been summarised in Figure 13 and the thin layer of fines observed at the top of the column has been plotted as a layer with 100% fines. From the grading curves and final distribution of fines throughout the column in Figures 12 and 13, it is evident that the material at the top of the column was finer than the material towards the bottom of the column. There was also more variation in the fines content in the layers of the well-graded material containing 28% fines than 18% fines.

The movement of fines throughout these well-graded materials is not unexpected. The flow of water through soils is known to cause fines within the material to migrate and this process, termed suffosion, is an internal stability phenomenon in which fine particles are transported through a non-plastic soil, resulting in the collapse of the soil structure (Chapuis, 1992; Fannin et al., 2014). For suffosion to occur, the hydraulic gradient needs to exceed a critical value and the soil itself needs to be unstable. Both requirements have been found to depend on the grading of the soil (Kenny et al., 1985, Li & Fannin, 2008, 2012, Hunter & Bowman, 2018). In this study, the pore pressure build-up measured during shaking resulted in hydraulic gradients close to the critical values required for suffosion to occur. The well graded materials containing 18% and 28% fines can also be classified as potentially unstable soils (Kezdi, 1979; Kenny et al., 1985) and they are similar in grading to materials which have demonstrated suffosion (Kenny et al., 1985; Li, 2008).

As already noted during the shaking of the well-graded materials the soil columns settled significantly, the fines accumulated at the column surface, and the final water level was at, or just above, the soil surface. Allowing for the settlement enables the average post-shaking void ratios ($e_{average}$) and degrees of saturation ($S_{r,corrected}$) to be calculated as reported in Table 2. It can be seen that significant decreases in void ratio have occurred and the final relative densities ($D_{r,final}$) are apparently well above 1. Given that all the initially unsaturated material had liquefied the average degrees of saturation would be expected to be between 0.9 and 1 and this is confirmed by the values in Table 2. However, if the final degrees of saturation are calculated from the local moisture contents for the well-graded material with 28% fines using the final average void ratios ($e_{average}$) and a constant value for specific gravity of 2.82, unreasonable degrees of saturation are calculated ($S_{r,calculated}$), as indicated in Table 3. Values greater than 1 result at the top of the soil column and unreasonably low values are estimated at the base. More reasonable degrees of saturation, within $\pm$2% of the measured final global degrees of saturation ($S_{r,corrected}$), can be determined if the inhomogeneity within the soil column is considered. The distribution of fines within the column was used to estimate the local specific gravities, which varied with fines migration because the specific gravities of feldspar fines and coarser basalt were 2.6 and 2.9, respectively. Assuming a constant degree of saturation throughout the column, within $\pm$2% of the measured global value, the local void ratios could be calculated from the moisture contents measured at the top, middle and bottom of the column. These calculated void ratios are included in Table 3, labelled as e, and the distribution of void ratios with column depth have been plotted in Figure 14. As expected, the void ratios were higher towards the top of the column. To estimate the void ratio of the thin, close to fully saturated layer of fines at the top of the soil column, a known mass of dry fines was pluviated into a measuring cylinder filled with water. The fines were left to settle for a few hours until the height of the settled and submerged fines layer could be accurately measured.

It is evident that the void ratio of the fines is significantly higher than estimated for the well-graded material. A weighted average ($e_{average}$) of the calculated local void ratios, based on the approximate thicknesses of the soil layers, as shown in Figure 15, was calculated in Table 3, to check the reasonableness of the calculated void ratios. These values are close to the global average values given in Table 2 and are not particularly sensitive to uncertainty in the thicknesses of the soil layers. This analysis suggests that it is reasonable to assume a constant degree of saturation throughout the liquefied column, and this is associated with densification at the base of the column, loosening at the top, upwards fines migration and the development of a loose fines layer on the column surface. It may also be noted that the presence of fines on the surface also reduced the permeability and contributed to keeping the soil in a liquefied state until shaking of the soil stopped.

3.3 Application of the findings and limitations

The results presented in this paper describe the fundamental liquefaction behaviour of unsaturated well graded materials, which are widely used as fill materials, in railway ballast and as pavement materials. The well graded materials also have gradings within the range of liquefiable shipped metallic cargoes. These tests have clearly demonstrated the potential for large settlements, fines migration and the development of very low effective stresses within a large number of cycles and at the amplitudes thought to be relevant for ships passing through storms. However, they have been conducted in a column of 0.5m height, with vertical excitation at a very high frequency of 50 Hz, which is more relevant to cyclic loading conditions on train ballast and highway pavements. Nevertheless, cyclic triaxial tests performed on the same well-graded unsaturated material showed similar trends in settlement accumulation and rapid pore pressure build up at lower frequencies when drainage was prevented (Kwa & Airey, 2019). Similar trends in pore pressures have also been observed in shake table tests performed on saturated and partially saturated sands that have liquefied, when cyclically loaded at lower, more realistic frequencies of between 0.1 to 8 Hz (Yegain et al., 2006, 2007; Ueng et al., 2006, 2010, 2017; Pathak et al., 2010, 2013). Although similar trends in behaviour may be observed, the susceptibility to liquefaction of the partially saturated well graded materials would be difficult to predict with existing models and understanding and there is a need for more well controlled and instrumented tests to develop and validate models.

The shake table used in this study is normally used to perform maximum density tests according to AS1289.5.5.1. (Similar to ASTM D4253). The minimum and maximum densities for the well graded materials tested in this study were also determined according to the standard AS1289.5.5.1, however, according to the standard, maximum density tests should not be performed on materials containing non-plastic fine contents greater than 12% (15% in ASTM D4253) because the fines can segregate. This was observed during the column tests in the well-graded materials containing 18% and 28% fines. Once the fines migrate, the material is no longer homogeneous and the measured global density in the column, which is significantly taller than the standard container used in the maximum density tests, is not representative of the local densities throughout the material. This resulted in an overestimation of the true relative densities of the material. It can be anticipated that tests to measure maximum density using wet samples that satisfy suffosion criteria for unstable soils are likely to be affected by fines migration and lead to unreliable maximum density values. The need for improved standards to measure maximum dry unit weight has recently been discussed (Lunne et al., 2019) and from our column tests it appears that tests should be performed dry to avoid internal instability.

4. CONCLUSION

This study investigated the cyclic unsaturated liquefaction responses of columns of loosely compacted well-graded materials that contain a wider range of particle sizes than more commonly tested sands and silty sands, and that have similar gradings to other soils that have been known to liquefy. Liquefaction was observed in all of the shake table tests performed on the well-graded materials containing 18 and 28% fines and prepared at degrees of saturation ranging from 50 to 70%. Prior to shaking moisture redistributed, decreasing at the surface and increasing at the base. When shaking started large settlements were observed in the upper partly saturated part of the column, whereas at the base very little settlement occurred and a saturation front could be seen to move upwards. As shaking continued the saturation front moved up to the column surface and the pore pressures increased to equal the total stress and the soil reached a liquefied state. The liquefied state was reached first at the bottom of the column, partly as a result of air in the upper parts restricting water flow, and settlement in the lower part of the column did not occur until the saturation front reached the surface. The fines in the well-graded materials also migrated towards the surface of the column due to the upward hydraulic gradient. Due to the migration of water and fines, the soil in the column was not homogeneous and as a result, the local densities also varied. The void ratios were found to increase at the top and decrease at the bottom.

The shake table used in this study vibrated in a vertical direction at higher frequencies and for a larger number of cycles than typically used in normal seismic liquefaction studies. This paper reports data and findings which are useful for understanding the fundamental cyclic liquefaction behaviour of unsaturated well graded materials when subjected to similar vertical cyclic loading conditions including during repetitive transport loading or in cargoes during shipping transportation. In addition to this, the data can also be used to validate finite element numerical models with dynamic unsaturated constitutive models that seek to predict the response of unsaturated soils to dynamic events.

5. ACKNOWLEDGEMENTS

The authors acknowledge the support provided by the Australian Research Council Discovery Scheme (grant DP150103083).

REFERENCES

Alobaidi, I. and Hoare, D.J., 1996. The development of pore water pressure at the subgrade-subbase interface of a highway pavement and its effect on pumping of fines. Geotextiles and geomembranes, 14(2), pp.111-135.

Andrus, R. (1995). In situ characterization of gravelly soils that liquefied in the 1983 Borah peak earthquake (Idaho). PhD thesis, University of Texas at Austin.

ASTM (2012). ASTM Designation D4253 Standard Test Methods for Maximum Index Density and Unit Weight of Soils Using a Vibratory Table. American Society for Testing and Materials

Bouckovalas, G. D., Andrianopoulos, K. I., and Papadimitriou, A. G. (2003). A critical state interpretation for the cyclic liquefaction resistance of silty sands. Soil Dynamics and Earthquake Engineering, 23(2):115–125.

Bowman, E., & Hunter, R. P. (2017). Visualisation of seepage induced suffusion and suffosion within internally erodible granular media. Géotechnique.

Campbell, G.S. (2001). Callibration and evaluation of the low-cost EC-5 soil moisture sensor. Retrieved from metergroup.com/environmental/articles/callibration-evaluation-ec-5-soil-moisture-sensor

Carrera, A., Coop, M. R., & Lancellotta, R. (2011). Influence of grading on the mechanical behaviour of Stava tailings. Géotechnique, 61(11), 935.

Chapuis, R. P. (1992). Similarity of internal stability criteria for granular soils. Canadian Geotechnical Journal, 29(4):711–713.

Cubrinovski, M., & Ishihara, K. (2003). Liquefaction-induced ground deformation and damage to piles in the 1995 Kobe Earthquake.

Cubrinovski, M., Bray, J., de la Torre, C., Olsen, 4. M., Bradley, B., Chiaro, G., ... & Wotherspoon, L. (2017). Liquefaction effects and associated damages observed at the Wellington Centreport from the 2016 Kaikoura earthquake.

Dash, H. and Sitharam, T. (2009). Undrained cyclic pore pressure response of sand–silt mixtures: effect of nonplastic fines and other parameters. Geotechnical and Geological Engineering, 27(4):501–517.

Duku, P. M., Stewart, J. P., Whang, D. H., & Yee, E. (2008). Volumetric strains of clean sands subject to cyclic loads. Journal of geotechnical and geoenvironmental engineering, 134(8), 1073-1085.

Duong, T.V., Cui, Y.J., Tang, A.M., Dupla, J.C., Canou, J., Calon, N. and Robinet, A., 2014. Investigating the mud pumping and interlayer creation phenomena in railway sub-structure. Engineering Geology, 171, pp.45-58.

Ebrahimi, A., Tinjum, J.M. and Edil, T.B., 2015. Deformational behavior of fouled railway ballast. Canadian Geotechnical Journal, 52(3), pp.344-355.

Fannin, R. and Slangen, P. (2014). On the distinct phenomena of suffusion and suffosion. Géotechnique Letters, 4(4):289–294.

Ghayoomi, M., & McCartney, J. S. (2011). Measurement of small-strain shear moduli of partially saturated sand during infiltration in a geotechnical centrifuge. Geotechnical Testing Journal, 34(5), 503-513.

Ghayoomi, M., McCartney, J. S., & Ko, H. Y. (2012). Empirical methodology to estimate seismically induced settlement of partially saturated sand. Journal of Geotechnical and Geoenvironmental Engineering, 139(3), 367-376.

Harder, JR, L. F. (1997). Application of the Becker Penetration Test for evaluating the liquefaction potential of gravelly soils. Technical report.

Hu, Y. (2017). Liquefaction of unsaturated soil under cyclic loading. Bachelor's thesis, The University of Sydney.

IMSBC, (2013). International maritime solid bulk cargoes code. International Maritime Organization.

Indraratna, B., Salim, W., Rujikiatkamjorn, C., 2011. Advanced Rail Geotechnology - Ballasted Track, CRC Press.

Ju, L., Vassalos, D., & Boulougouris, E. (2016). Numerical assessment of cargo liquefaction potential. Ocean Engineering, 120, 383-388.

Kenny, T. and Lau, D. (1985). Internal stability of granular soils. Canadian Geotechnical Journal, 21:634–643.

Kezdi, A. (1979). Soil physics – selected topics. Amsterdam, the Netherlands: Elsevier Scientific Publishing Co.

Kimoto, S., Oka, F., Fukutani, J., Yabuki, T., and Nakashima, K. (2011). Monotonic and cyclic behaviour of unsaturated sandy soil under drained and fully undrained conditions. Soils and foundations, 51(4):663–681.

Kokusho, T. (1999). Water film in liquefied sand and its effect on lateral spread. Journal of Geotechnical and Geoenvironmental Engineering, 125(10), 817-826.

Kokusho, T., & Kojima, T. (2002). Mechanism for postliquefaction water film generation in layered sand. Journal of geotechnical and geoenvironmental engineering, 128(2), 129-137.

Kwa, K. A., & Airey, D. W. (2017). Effects of fines on liquefaction behaviour in well-graded materials. Canadian Geotechnical Journal, 54(10), 1460-1471.

Kwa, K. A., & Airey, D. W. (2019).Effects of fines on the cyclic liquefaction behaviour in unsaturated, well-graded materials. Soils and Foundations

Li, M., & Fannin, R. J. (2008). Comparison of two criteria for internal stability of granular soil. Canadian Geotechnical Journal, 45(9), 1303-1309.

Li, M., & Fannin, R. J. (2012). A theoretical envelope for internal instability of cohesionless soil. Géotechnique, 62(1), 77-80.

Lunne, T., Knudsen, S., Blaker, O., Vestgarden, T., Powell, J.J.M., Wallace, C.F., Krogh, L., Thomson N.V., Yetginer, G., and Ghanekar, R.K. (2019) Methods used to determine maximum and minimum dry unit weights of sand: Is there a need for a new standard? Canadian Geotechnical Journal, 56: 536-553

Munro, M. C. and Mohajerani, A. (2016). Moisture content limits of iron ore fines to prevent liquefaction during transport: review and experimental study. International Journal of Mineral Processing, 148:137–146.

Okamura, M. and Soga, Y. (2006). Effects of pore fluid compressibility on liquefaction resistance of partially saturated sand. Soils and Foundations, 46(5):695–700.

Özener, P. T., Özaydın, K., & Berilgen, M. M. (2009). Investigation of liquefaction and pore water pressure development in layered sands. Bulletin of Earthquake Engineering, 7(1), 199-219.

Pathak, S. R., Dalvi, R. S., & Katdare, A. D. (2010). Earthquake Induced Liquefaction using Shake Table Test.

Pathak, S. R., Kshirsagar, M. P., & Joshi, M. S. (2013). Liquefaction triggering criterion using shake table test. Int. J. Eng. Tech, 5, 4439-4449.

Polito, C. P. and Martin II, J. R. (2001). Effects of nonplastic fines on the liquefaction resistance of sands. Journal of Geotechnical and Geoenvironmental Engineering, 127(5):408–415.

Proceedings of the 6th International Symposium on Deformation Characteristics of Geomaterials, IS-Buenos Aires 2015, 15-18 November 2015, Buenos Aires, Argentina, volume 6, page 299. IOS Press.

Report 3, Technical Working Group (TWG).

Sadek, S. and Saleh, M. (2007). The effect of carbonaceous fines on the cyclic resistance of poorly graded sands. Geotechnical and Geological Engineering, 25(2):257.

Sadrekarimi, A. (2013). Influence of fines content on liquefied strength of silty sands. Soil Dynamics and Earthquake Engineering, 55:108–119.

Stewart, J. P., & Whang, D. H. (2003). Simplified procedure to estimate ground settlement from seismic compression in compacted soils. In Proc. 2003 Pacific Conference on Earthquake Engineering.

Tehrani, K. (2016). Developing a new instrumented soil column to study climate-induced ground movement in expansive soil (Doctoral dissertation, Queensland University of Technology).

Tsuchida, H. (1970). Prediction and countermeasure against the liquefaction in sand deposits. In Abstract of the seminar in the Port and Harbor Research Institute, pages 31–333.

TWG (2013). TWG 3rd report and Imperial College review- Proctor Fagerberg (PF) Test.

Ueng, T. S., Wang, M. H., Chen, M. H., Chen, C. H., & Peng, L. H. (2006). A large biaxial shear box for shaking table test on saturated sand. Geotechnical Testing Journal, 29(1), 1-8.

Ueng, T. S., Wang, Z. F., Chu, M. C., & Ge, L. (2017). Laboratory tests for permeability of sand during liquefaction. Soil Dynamics and Earthquake Engineering, 100, 249-256.

Ueng, T. S., Wu, C. W., Cheng, H. W., & Chen, C. H. (2010). Settlements of saturated clean sand deposits in shaking table tests. Soil Dynamics and Earthquake Engineering, 30(1-2), 50-60.

Unno, T., Kazama, M., Sento, N., and Uzuoka, R. (2006). Cyclic shear behavior of unsaturated volcanic sandy soil under various suction conditions. In Unsaturated Soils 2006, pages 1133–1144.

Unno, T., Kazama, M., Uzuoka, R., and Sento, N. (2008). Liquefaction of unsaturated sand considering the pore air pressure and volume compressibility of the soil particle skeleton. Soils and Foundations, 48(1):87–99.

Uzuoka, R., Unno, T., Sento, N., and Kazama, M. (2014). Effect of pore air pressure on cyclicbehavior of unsaturated sandy soil. In Proceedings of the 6th International Conference on Unsaturated Soils, UNSAT, pages 783–789.

Wang, H., Koseki, J., Sato, T., and Tantian, J. (2015). Experimental evaluation of liquefaction resistance of unsaturated sandy soils. In Deformation Characteristics of Geomaterials:

Xenaki, V. and Athanasopoulos, G. (2003). Liquefaction resistance of sand–silt mixtures: an experimental investigation of the effect of fines. Soil Dynamics and Earthquake Engineering, 23(3):1–12.

Yanagisawa, E., & Jafarzadeh, F. (1995). Behaviour of Saturated Sand Models under Principal Stress Axes Rotation in Shake Table Tests.

Yegian, M. K., Eseller, E., & Alshawabkeh, A. (2006). Preparation and cyclic testing of partially saturated sands. In Unsaturated Soils 2006 (pp. 508-518).

Yegian, M. K., Eseller-Bayat, E., Alshawabkeh, A., & Ali, S. (2007). Induced-partial saturation for liquefaction mitigation: experimental investigation. Journal of Geotechnical and Geoenvironmental Engineering, 133(4), 372-380.

TABLES

Table 1: Material parameters

Material	ϕ_{cs} (°)	G_s	e_{min}	e_{max}
Sydney Sand	32	2.65	0.60	0.81
Feldspar Fines	37	2.6	0.38	0.57
Well-Graded 18% Fines	42	2.85	0.34	0.52
Well-Graded 28% Fines	40	2.82	0.39	0.72

Table 2: Summary of shake table tests and the average moisture and density state values

Name	Material	$e_{initial}$	$Dr_{initial}$	$mc_{initial}$	$Sr_{initial}$	e_{final}	Sr_{final}	Dr_{final}
SydSSr29	Sydney Sand	0.82	-0.05	0.09	0.29	No Change		
SydSSr56	Sydney Sand	0.57	1.15	0.12	0.56	No Change		
SydSS68	Sydney Sand	0.60	0.7	0.17	0.68	No Change		
18Sr50	18% Fines	0.51	0.06	0.088	0.50	0.3	0.84	1.22
18Sr60	18% Fines	0.43	0.53	0.089	0.60	0.27	0.96	1.39
18Sr70	18% Fines	0.38	0.78	0.093	0.71	0.275	0.97	1.36
28Sr56	28% Fines	0.55	0.52	0.11	0.56	0.34	0.91	1.15
28Sr60	28% Fines	0.54	0.55	0.115	0.60	0.34	0.95	1.15
28Sr60b	28% Fines	0.51	0.63	0.107	0.60	0.31	0.96	1.24
28Sr62	28% Fines	0.51	0.64	0.115	0.62	0.34	0.95	1.15
28Sr65	28% Fines	0.50	0.67	0.115	0.65	0.34	0.95	1.15
28Sr72	28% Fines	0.45	0.81	0.115	0.72	0.34	0.95	1.15

Table 3: Summary of the final moisture contents, degrees of saturation and void ratios at the top, middle and bottom of the column of the well-graded material with 28% fines

Name	Layer	$m_{c,meausred}$	$S_{r,calculated}$	G_s	Layer thickness	e	$S_{r,corrected}$
28Sr56	fines	-	-	2.60	10	1.5	-
	top	0.112	0.902	2.77	82.5	0.34	0.912
	middle	0.109	0.878	2.80	130	0.33	0.925
	bottom	0.1	0.806	2.82	187.5	0.31	0.911
					$e_{average}$	0.351	
28Sr60	fines	-	-	2.60	10	1.5	-
	top	0.125	1.037	2.78	82.5	0.36	0.965
	middle	0.105	0.871	2.80	130	0.31	0.948
	bottom	0.1	0.829	2.82	187.5	0.3	0.941
					$e_{average}$	0.345	
28Sr62	fines	-	-	2.60	10	1.5	-
	top	0.125	1.037	2.78	82.5	0.36	0.979
	middle	0.12	0.995	2.80	130	0.34	0.988
	bottom	0.11	0.912	2.82	187.5	0.31	0.995
					$e_{average}$	0.359	
28Sr65	fines	-	-	2.60	10	1.5	-
	top	0.13	1.078	2.78	82.5	0.37	0.977
	middle	0.11	0.912	2.80	130	0.32	0.963
	bottom	0.105	0.871	2.82	187.5	0.31	0.956
					$e_{average}$	0.354	
28Sr72	fines	-	-	2.60	10	1.5	-
	top	0.125	1.037	2.77	82.5	0.35	0.993
	middle	0.12	0.995	2.80	130	0.34	0.998
	bottom	0.102	0.829	2.82	187.5	0.30	0.941
					$e_{average}$	0.352	

FIGURES

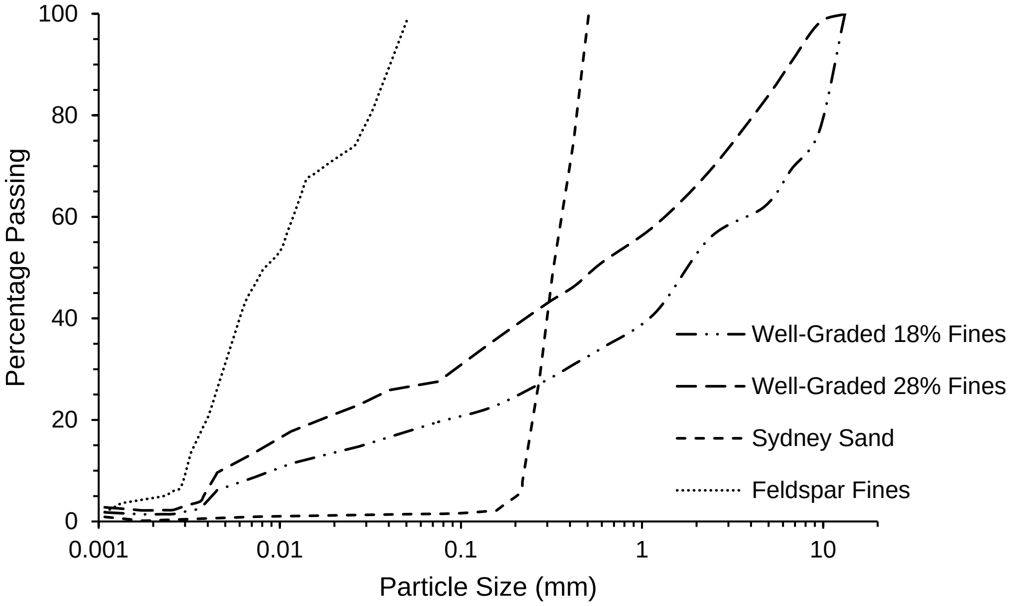

Figure 1: Grading curves

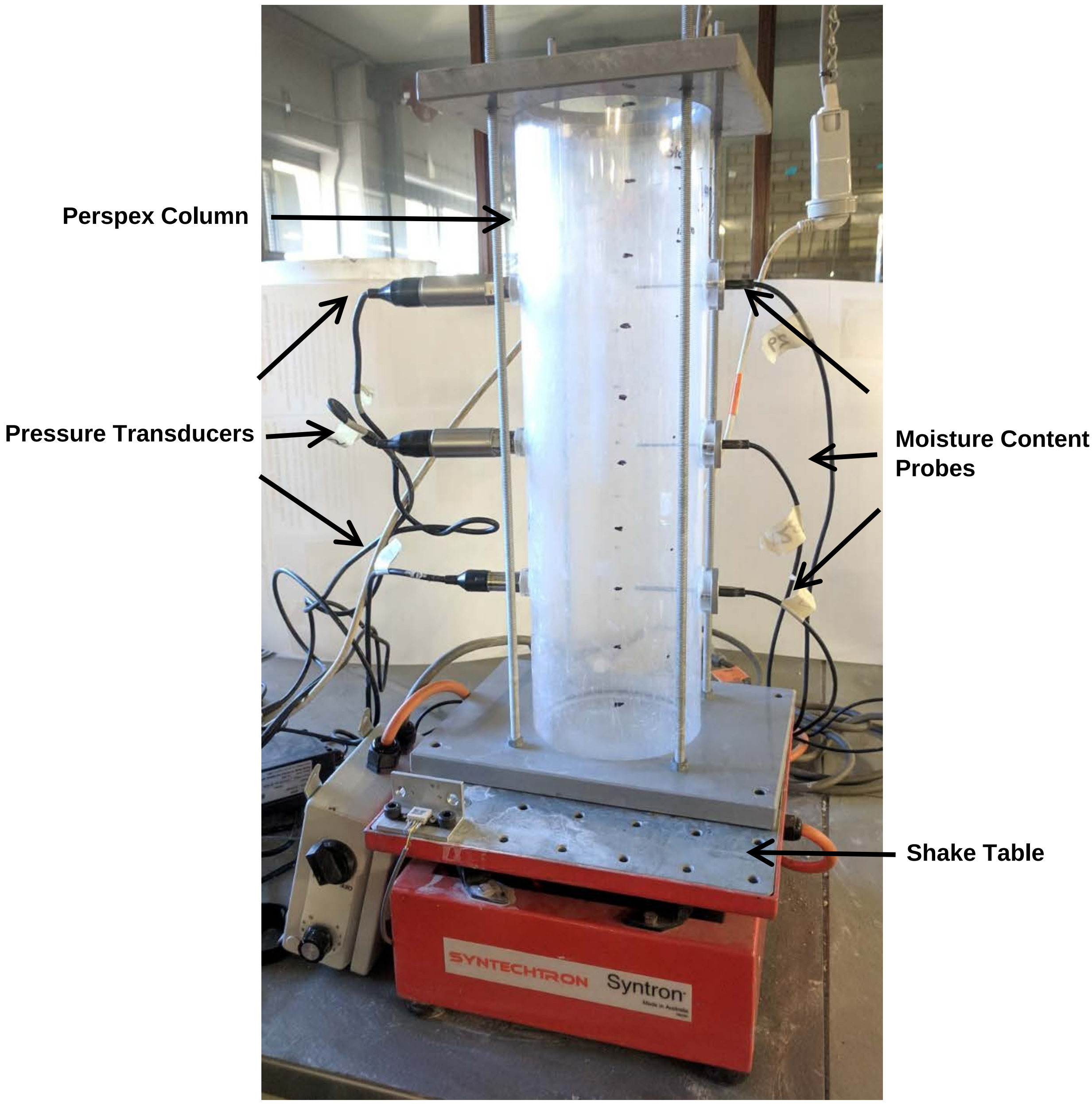

Figure 2: Shake table and soil column set up

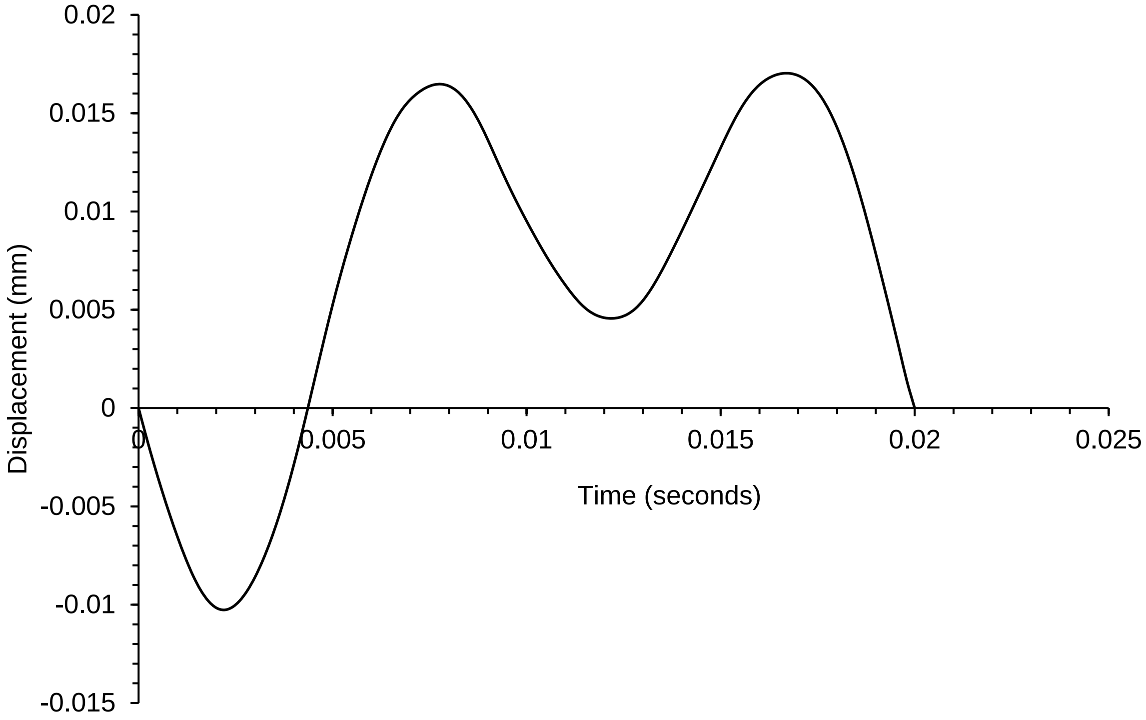

Figure 3: Typical displacement waveform produced by the shake table

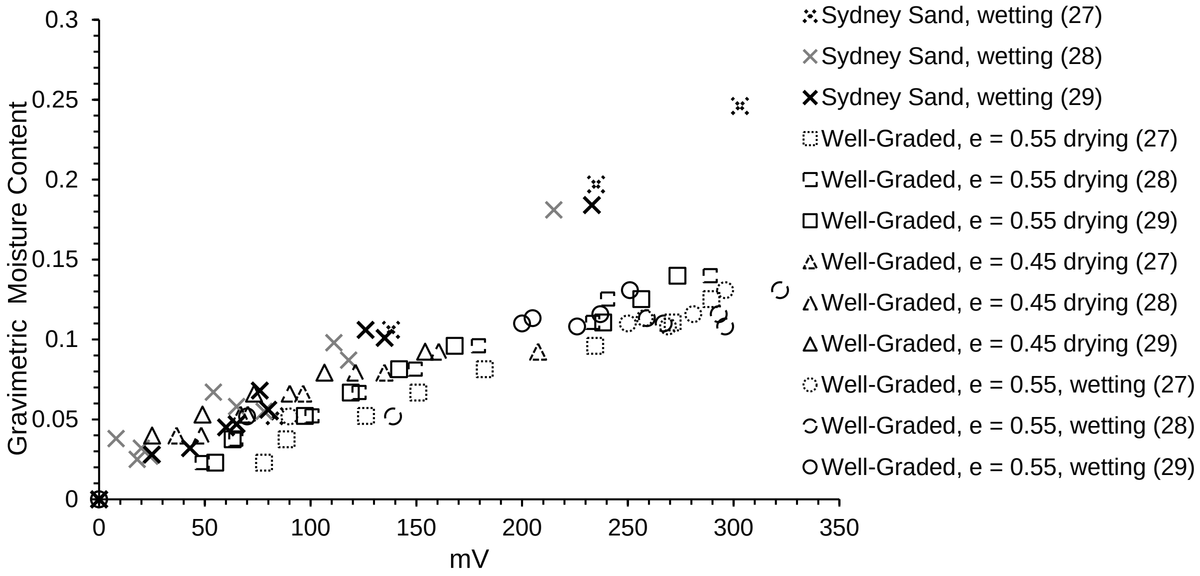

Figure 4: Calibration of moisture content probes

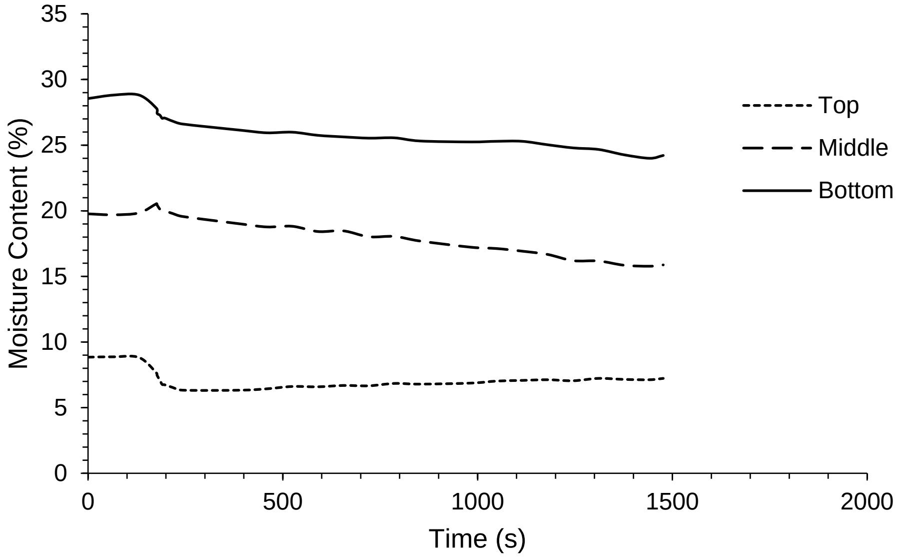

(a)

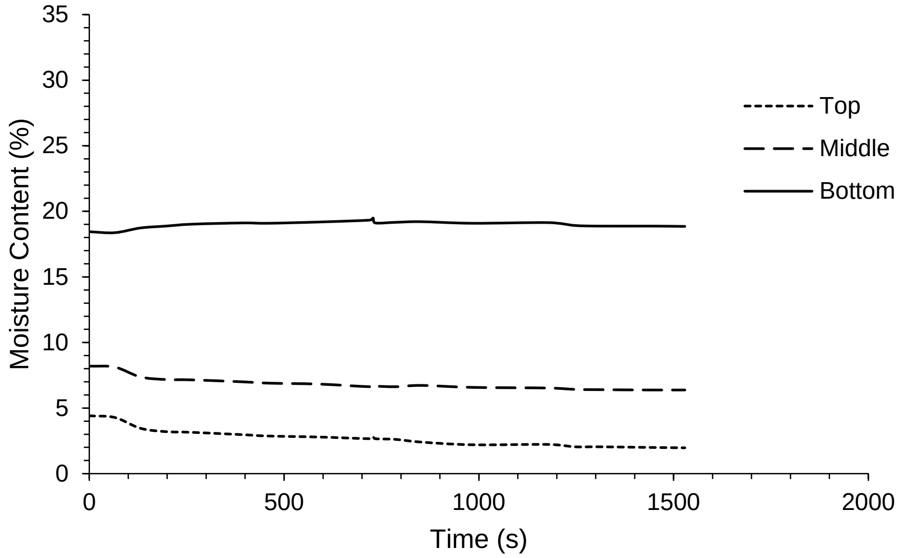

(b)

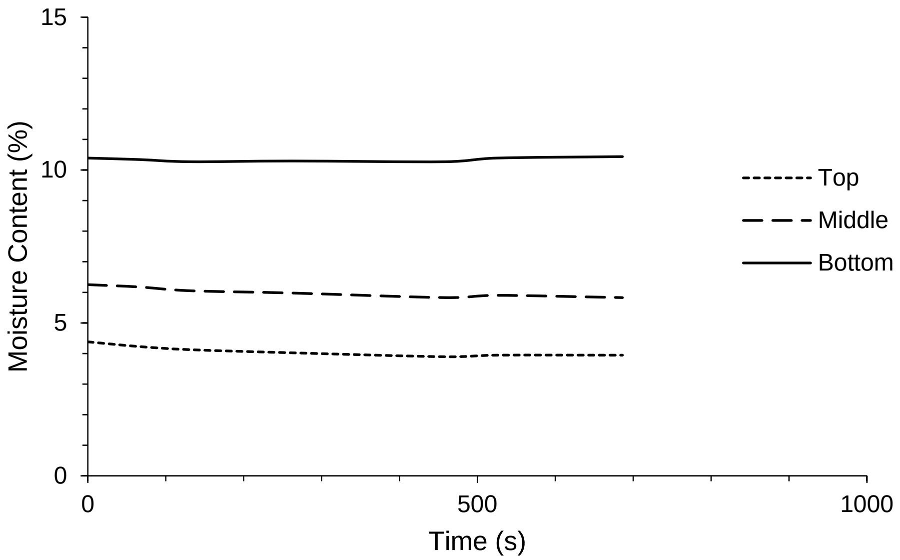

(c)

Figure 5: Moisture content measurements in sand for tests (a) SydSS68, (b) SydSS56 and (c) SydSS29

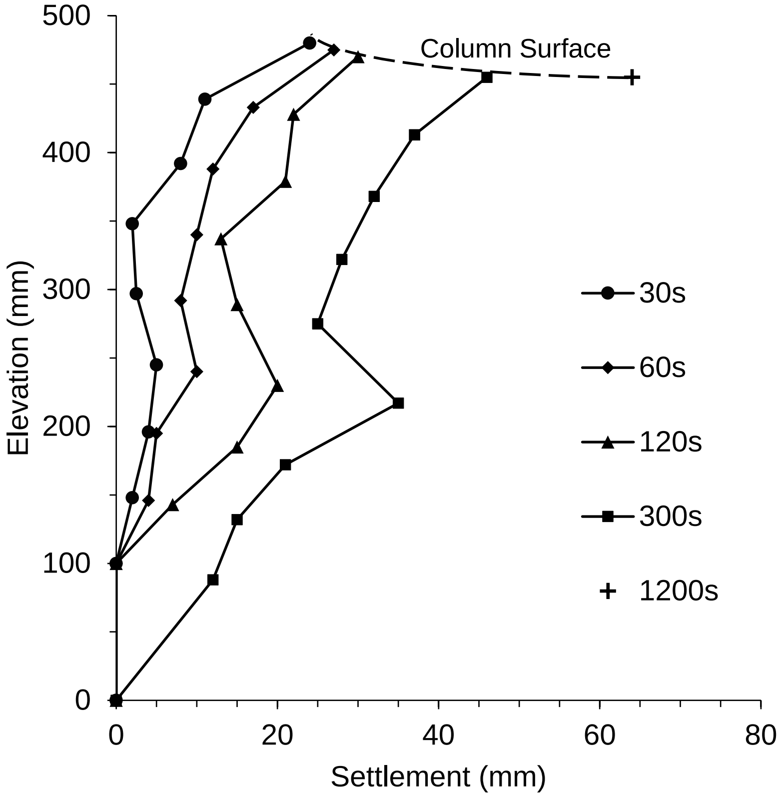

Figure 6: Change in settlement profiles during shaking (28Sr60b)

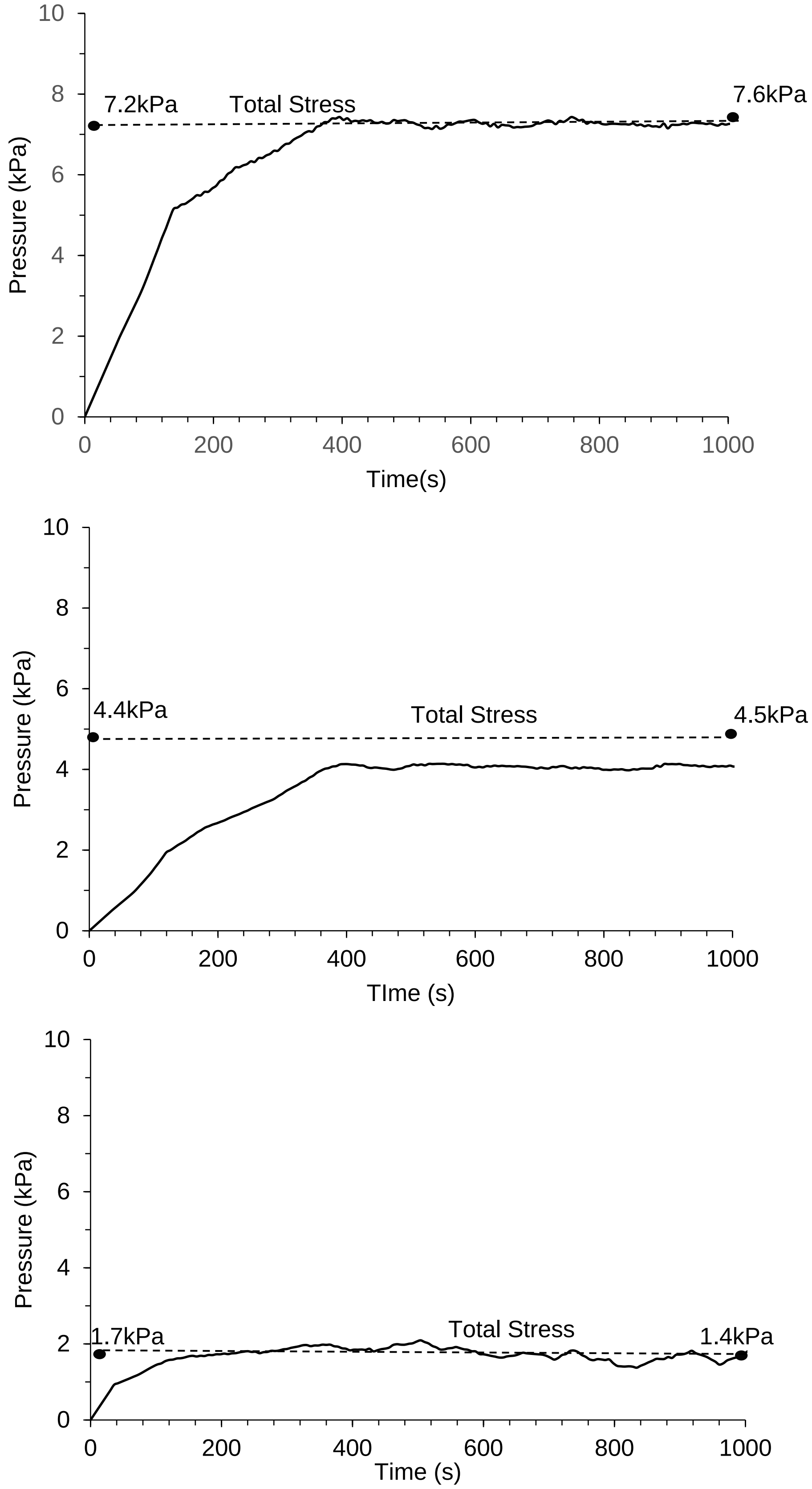

(a)

(b)

(c)

Figure 7: Typical pore pressures in the well-graded materials with 18% fines (18Sr70) measured at the (a) bottom, (b) middle and (c) top

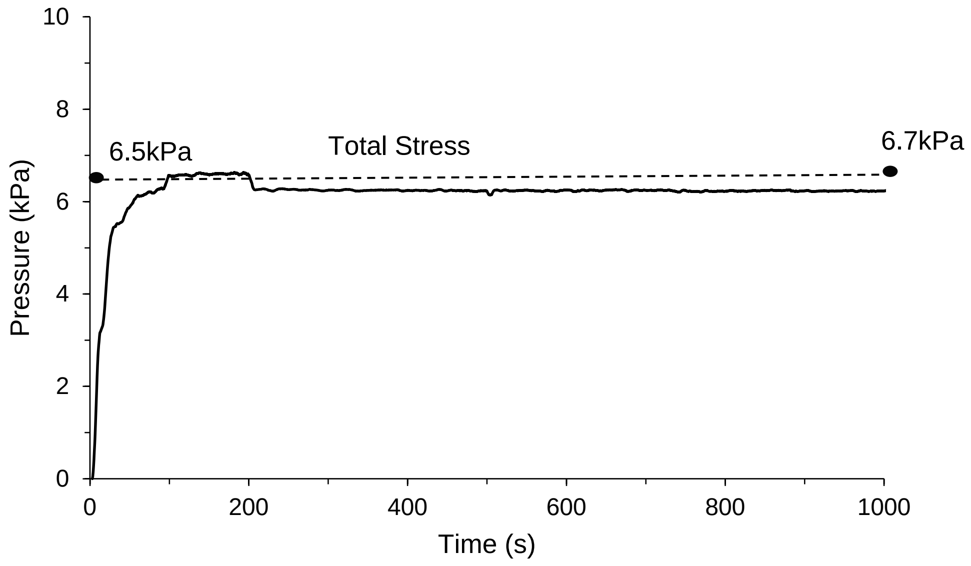

(a)

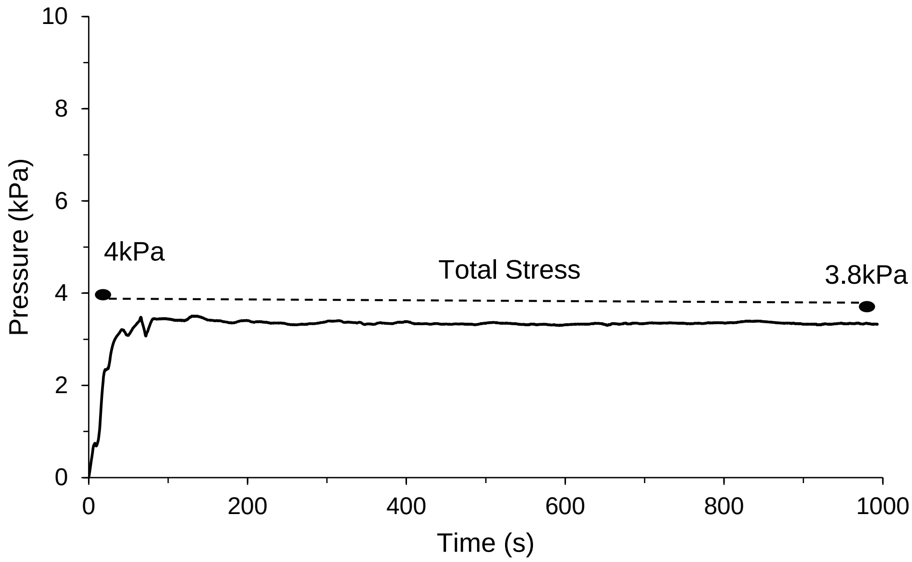

(b)

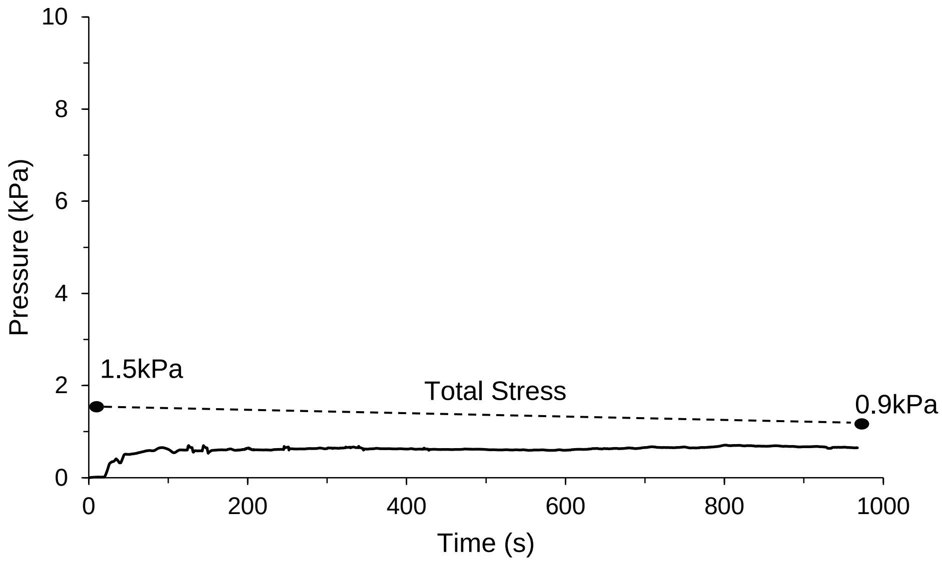

(c)

Figure 8: Typical pore pressures in the well-graded materials with 28% fines (28Sr62) measured at the (a) bottom, (b) middle and (c) top

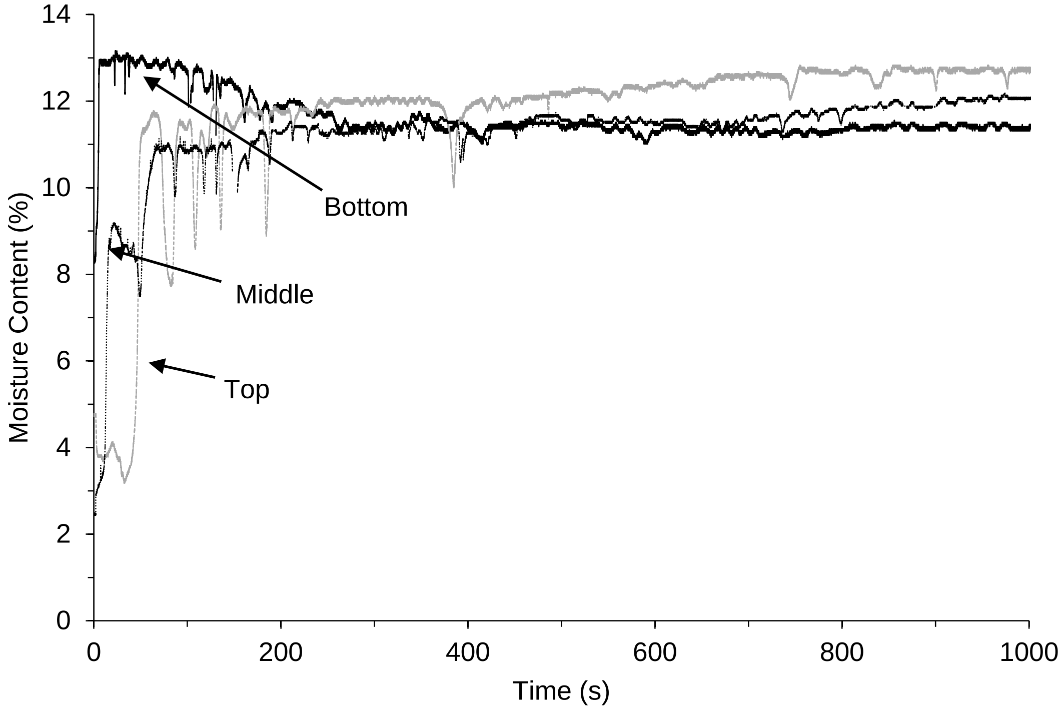

(a)

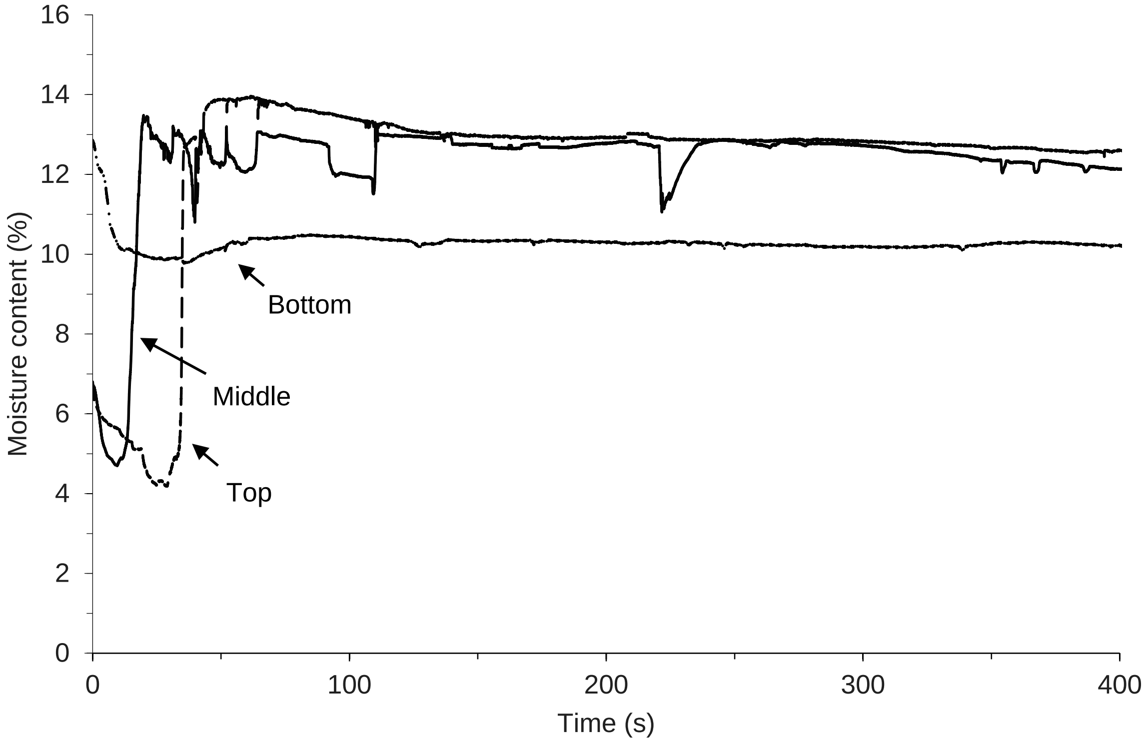

Figure 9: Comparison of moisture contents measured at the bottom, middle and top of samples (a) 28Sr62 and (b) 28Sr72

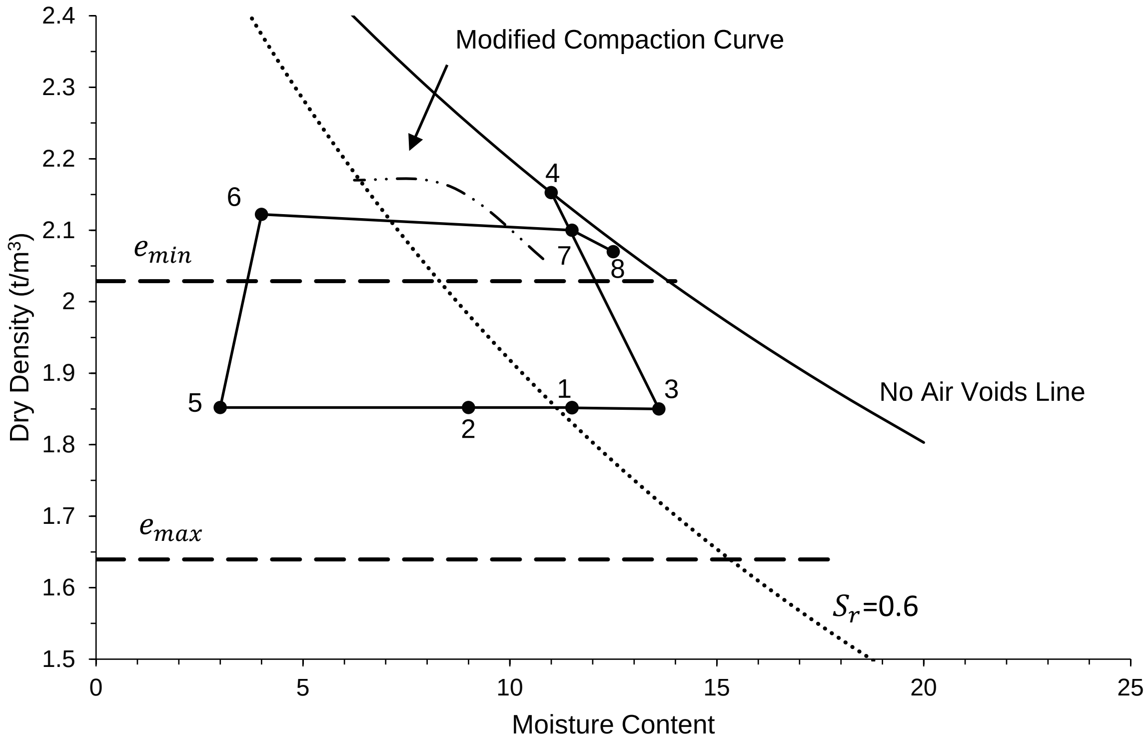

Figure 10 Schematic showing typical moisture and density paths at bottom and top moisture content probe locations during shaking (28Sr62).

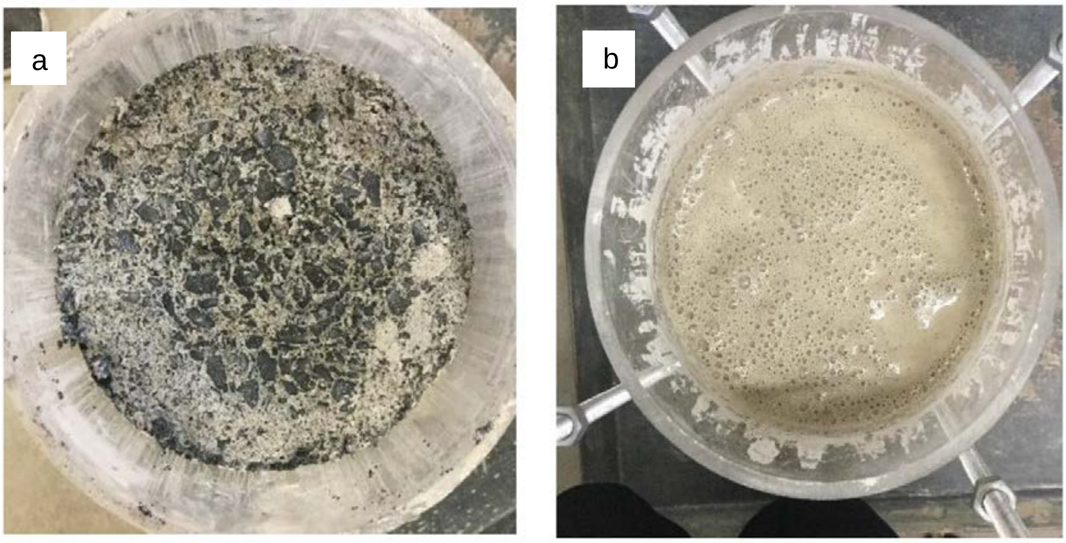

Figure 11: Photographs of the (a) bottom and (b) top of the column

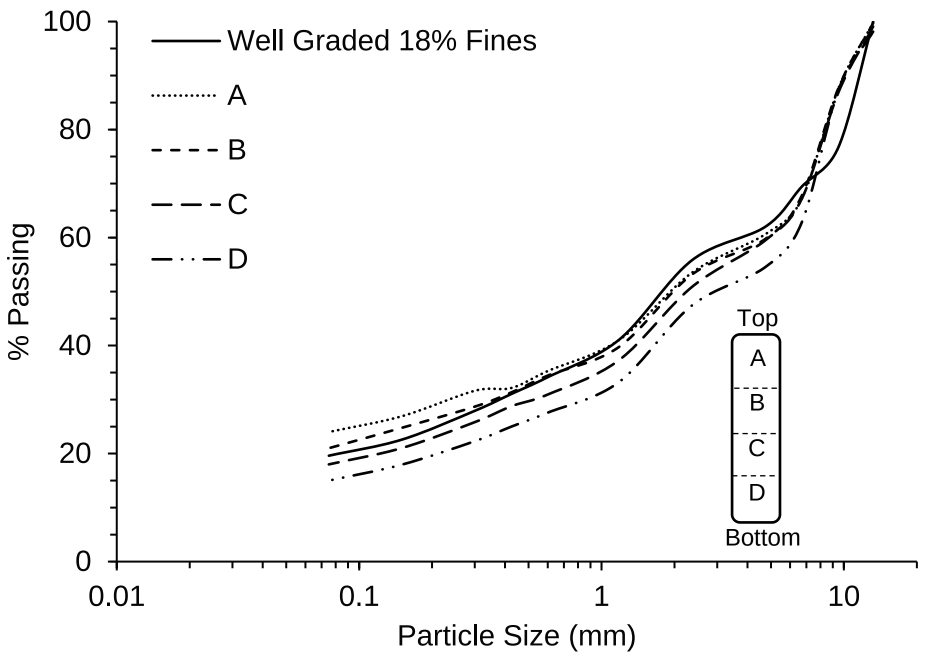

(a)

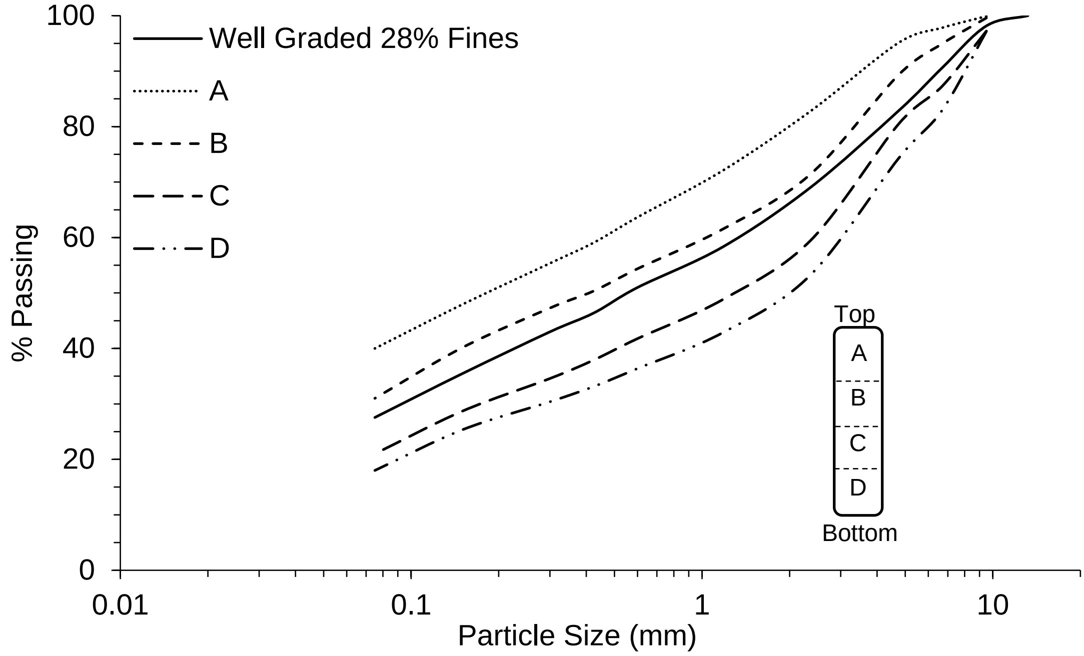

(b)

Figure 12: Sieve analysis performed on layers throughout the column containing the well-graded material with (a) 18% Fines and (b) 28% Fines

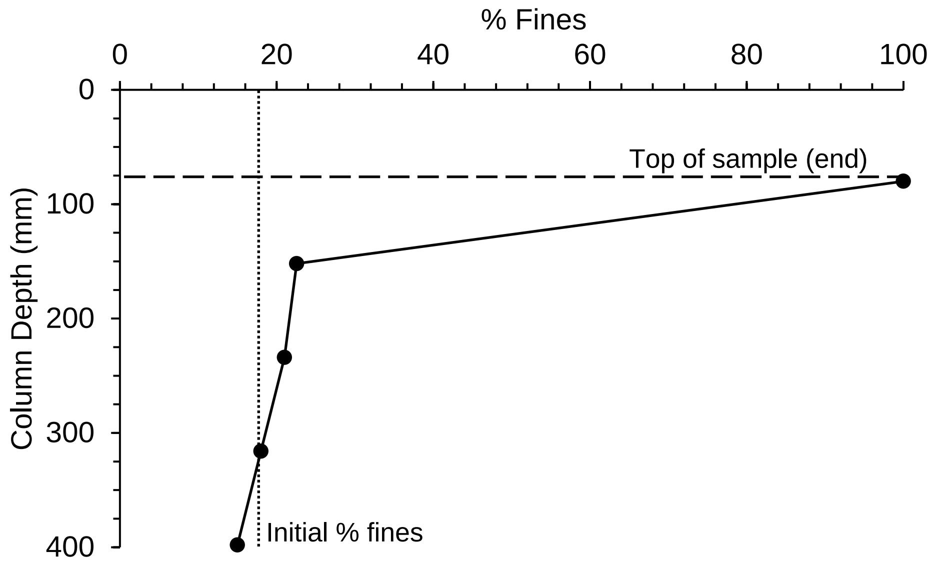

(a)

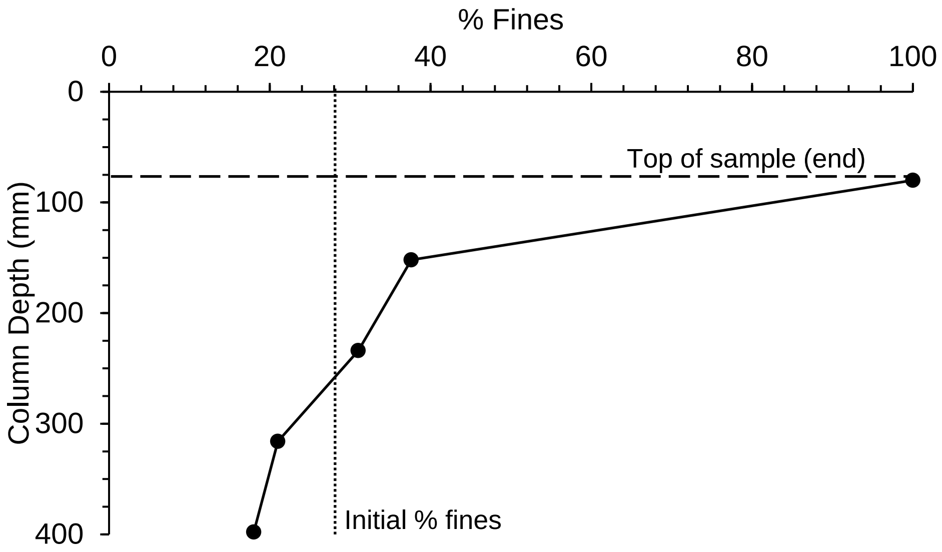

(b)

Figure 13: Typical distribution of fines throughout column after shaking in the well-graded materials containing (a) 18% fines and (b) 28% fines

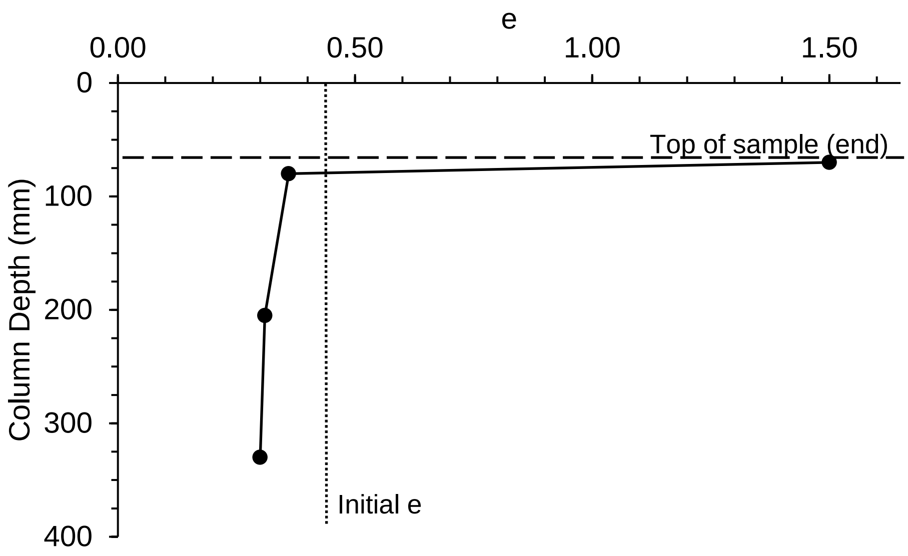

Figure 14: Typical distribution of the back calculated void ratios throughout column after shaking in the well-graded material containing 28% fines required to maintain a constant degree of saturation of within the column

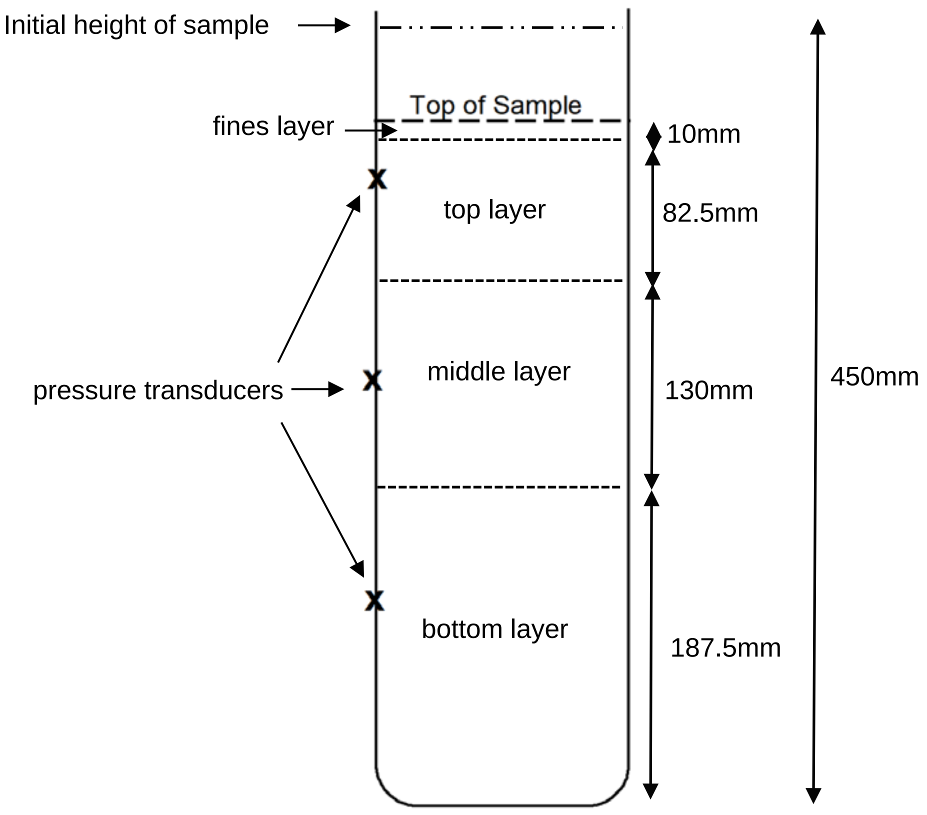

Figure 15: Diagram of column with dimensions of layers